

AD-A100 030

DEVELOPMENT OF A NOVEL LASER MATERIAL FOR MINIATURIZED
LASER SYSTEM(U) PHILIPS LABS BRIARCLIFF MANOR NY
W ZNICKER JUL 81 NDA903-81-C-0034

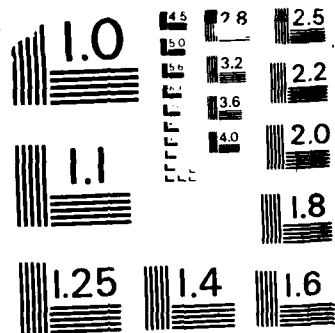
1/1

UNCLASSIFIED

F/G 9/3

NL





MICROCOPY RESOLUTION TEST CHART
NATIONAL BUREAU OF STANDARDS-1963-A

AD-A188 030

DEVELOPMENT OF A NOVEL LASER MATERIAL
FOR MINIATURIZED LASER SYSTEMS

QUARTERLY TECHNICAL REPORT

1 April to 30 June 1981

Sponsored by

DEFENSE ADVANCED RESEARCH PROJECTS AGENCY

DARPA Order No. 4040

Contract No. MDA903-81-C-0034

Principal Investigator: Dr. Walter Zwicker (914) 762-0300

Monitored by: Dr. Jefferey L. Paul

Contract Period: 8 Nov. 1980 - 31 Oct. 1982

THE VIEWS AND CONCLUSIONS CONTAINED IN THIS DOCUMENT
ARE THOSE OF THE AUTHORS AND SHOULD NOT BE INTERPRETED
AS NECESSARILY REPRESENTING THE OFFICIAL POLICIES,
EITHER EXPRESSED OR IMPLIED, OF THE DEFENSE ADVANCED
RESEARCH PROJECTS AGENCY OR THE UNITED STATES GOVERNMENT.

DTIC
ELECTE
DEC 03 1987
S
D
F

F

Prepared by

PHILIPS LABORATORIES
A Division of North American Philips Corporation
Briarcliff Manor, New York 10510

July 1981

87 11 18 078

20. ABSTRACT (Cont'd.)

emission cross sections of the Nd³⁺ ions in these crystals. Using the emission cross sections and the fluorescence lifetime values measured previously, rough comparisons were made of the laser performance parameters of the three crystals. Using the experimental laser setup described in the previous quarterly report, we obtained the output energy versus electrical input energy characteristics of the NdPP laser for various mirror and cavity configurations. Approximate efficiencies of the laser pumping system were calculated. Fabrication of a miniature laser with optimum output is being seriously hindered by the lack of proper-size miniature flash lamps (2-3 mm O.D. and 15-20 mm arc length). These lamps are no longer available from the previous supplier. While one request-for-quotation is still outstanding, to date no other company has been found that would be willing to produce lamps of this size.

PREFACE

This work is being performed by Philips Laboratories, a Division of North American Philips Corporation, Briarcliff Manor, New York under the overall supervision of Dr. Rameshwar Bhargava, Director, Exploratory Research Group. Dr. Walter Zwicker, Senior Program Leader for Crystal Growth and Materials Technology, is the Principal Investigator. Mr. Emil Abelaf and Mr. Theodore Kovats are responsible for crystal growing; Dr. Sel Colak and Mr. Jacob Khurgin are responsible for materials evaluation as well as laser design and construction.

This program is sponsored by the Defense Advanced Research Projects Agency (DARPA) and was initiated under Contract No. MDA903-81-C-0034. Dr. Jefferey L. Paul is the Contracting Officer's Technical Representative for DARPA.

The work described in this third Quarterly Technical Report covers the period from 1 April to 30 June 1981.

Accession for	
NTIS GRA&I	<input checked="" type="checkbox"/>
DTIC TAB	<input checked="" type="checkbox"/>
Unannounced	<input type="checkbox"/>
Justification	
By _____	
Distribution/	
Availability Codes	
Dist	Avail. and/or Special
A-1	



SUMMARY

Growth experiments have continued on crystals of $\text{NdP}_5\text{O}_{14}$ (NPP) and $\text{NdLiP}_4\text{O}_{12}$ (LNP). Laser rods are now being fabricated from large NPP crystals of excellent optical quality. Top-seeding experiments on LNP crystals produced single crystals up to 1 cm in size; however, the optical quality was poor, presumably due to inhomogeneities of the fluxed melt. The growth setup is being changed to overcome this problem. Emission spectra of Nd in NPP, LNP, and NAB crystals have been recorded at both room and liquid-nitrogen temperatures. Together with the absorption spectra, these measurements gave the emission cross sections of the Nd^{3+} ions in these crystals. Using the emission cross sections and the fluorescence lifetime values measured previously, rough comparisons were made of the laser performance parameters of the three crystals. Using the experimental laser setup described in the previous quarterly report, we obtained the output energy versus electrical input energy characteristics of the NdPP laser for various mirror and cavity configurations. Approximate efficiencies of the laser pumping system were calculated. Fabrication of a miniature laser with optimum output is being seriously hindered by the lack of proper-size miniature flash lamps (2-3 mm O.D. and 15-20 mm arc length). These lamps are no longer available from the previous supplier. While one request-for-quotation is still outstanding, to date no other company has been found that would be willing to produce lamps of this size.

TABLE OF CONTENTS

<u>Section</u>	<u>Page</u>
PREFACE.....	3
SUMMARY.....	4
LIST OF ILLUSTRATIONS.....	6
1. INTRODUCTION.....	7
2. MATERIALS PREPARATION AND CRYSTAL GROWTH.....	8
2.1 $\text{NdP}_5\text{O}_{14}$ (NPP).....	8
2.2 $\text{NdLiP}_4\text{O}_{12}$ (LNP).....	8
2.3 $\text{NdAl}_3(\text{BO}_3)_4$ (NAB).....	11
3. OPTICAL CHARACTERIZATION OF LASER MATERIALS.....	13
3.1 Emission Spectra.....	13
3.2 Emission Cross Sections.....	13
3.3 Basic Spectroscopic and Laser Properties of Crystals....	14
4. LASER PERFORMANCE OF NPP.....	24
5. PLANS FOR NEXT QUARTER.....	29
6. REFERENCES.....	29
DISTRIBUTION LIST.....	31

LIST OF ILLUSTRATIONS

<u>Figure</u>	<u>Page</u>
1. Growth temperature vs. lifetime for NPP crystals.....	9
2. Time vs. temperature for growth of NPP crystals.....	10
3. Pulling system for top-seeded flux growth of LNP crystals.....	12
4. LNP crystal grown by top-seeded flux growth method.....	12
5. Room-temperature emission spectrum of Nd ³⁺ in NPP. Peak emission wavelength is indicated. Value in parenthesis was taken from Ref. 1.....	16
6. Room-temperature emission spectrum of Nd ³⁺ in LNP. Peak emission wavelength is indicated. Value in parenthesis was taken from Ref. 2.....	17
7. Room-temperature emission spectrum of Nd ³⁺ in NAB. Peak emission wavelength is indicated. Value in parenthesis was taken from Ref. 3.....	18
8. Liquid-nitrogen temperature emission spectrum of Nd ³⁺ in NPP. The levels are assigned for the transitions from ⁴ F _{3/2} doublet to ⁴ I _{11/2} and ⁴ I _{9/2} multiplets in NPP.....	19
9. Liquid-nitrogen temperature emission spectrum of Nd ³⁺ in LNP....	20
10. Absorption spectrum of NPP near ⁴ I _{9/2} --> ⁴ F _{3/2} transition to be used in calculating emission cross section.....	21
11. Absorption spectrum of LNP near ⁴ I _{9/2} --> ⁴ F _{3/2} transition to be used in calculating emission cross section.....	22
12. Absorption spectrum of NAB near ⁴ I _{9/2} --> ⁴ F _{3/2} transition to be used in calculating emission cross section.....	23
13. Light output energy vs. electrical input energy for NPP laser in a double elliptical pumping cavity with two flash lamps and output mirror reflectivities of 75% and 85%.....	26
14. Light output energy vs. electrical input energy for NPP laser in a double elliptical pumping cavity with one flash lamp (failure mode) and output mirror reflectivities of 75% and 85%...	27
15. Light output energy vs. electrical input energy for NPP laser in a single elliptical cavity with 85% reflective output mirror..	28

1. INTRODUCTION

Growth experiments on crystals of NPP, LNP and NAB have continued. The previous crucible problem that was affecting the quality of the NPP crystals has been eliminated, and the optimum growth temperature has been established for crystals with maximum fluorescence life time and excellent optical quality. Top-seeded growth experiments on LNP crystals produced single crystals up to 1 cm in size; however, they were not free of inclusions.

Growth experiments on NAB crystals have been discontinued because of their poor quality and the possibility that the crystals might be dual-phase.

All three stoichiometric crystals of Nd^{3+} , namely NPP, LNP, and NAB, have been tested for their lasing properties. These properties are summarized, and their effects on laser threshold and output power are tabulated. Due to availability of larger size crystals, NPP seems to be the most suitable material for the miniature laser.

Extended measurements were made on the behavior of the NPP laser. The results indicate that the flash lamp used for pumping is inefficient at the low pulse energies of interest. This is reflected in the high threshold and output behavior of these NPP lasers.

2. MATERIAL PREPARATION AND CRYSTAL GROWTH

2.1 $\text{NdP}_5\text{O}_{14}$ (NPP)

Crystals of NPP, which are being grown by us on a routine basis, are still by far the largest and optically most perfect stoichiometric Nd laser crystals which have ever been produced. The problem with the shape of the crucible bottoms has been solved. Most of the newly purchased crucibles have the correct shape; those that do not are reshaped and repolished by us. As described in our last report, the crucible bottoms of certain shipments had been slightly convex, instead of flat, resulting in the growth of poor-quality crystals.

Since the lifetime of the $\text{Nd}^{3+} 4\text{F}_{3/2}$ fluorescence increases significantly with increasing growth temperature (Fig. 1) for NPP crystals, we studied this influence and determined, at the same time, the optimum, i.e., the maximum, permissible growth temperature. In our semi-sealed growth system (Ref. 1), two major factors determine the upper temperature limit for growth of NPP, viz., vapor pressure of the acid mixture and thermal stability of the vitreous carbon crucible. Too high a temperature and therefore too-high a vapor pressure leads to: severe losses of P_2O_5 (+ H_2O) and thereby multiple nucleation, poor-quality crystals, severe chemical attack of all quartz parts of the system, and severe thermal attack (oxidation) of the carbon crucible. In our system, there is a narrow temperature range in which crystals of NPP with a maximum fluorescence lifetime can be grown without reaching such conditions; this temperature range was determined to be between 550 and 590°C. Figure 2 shows the time and temperature for a NPP growth run under such "optimum" conditions. Laser rods 2 x 2 x 18 mm in size are now being fabricated from crystals of high optical quality which are being produced under such conditions.

2.2 $\text{NdLiP}_4\text{O}_{12}$ (LNP)

Crystals of LNP have to be grown from a fluxed solution. Most of the LNP crystals grown by this method inside such a flux, however, are of poor quality. Since top seeding appears to be the most promising technique, we have installed a crystal puller which allows seeding of the top of a fluxed

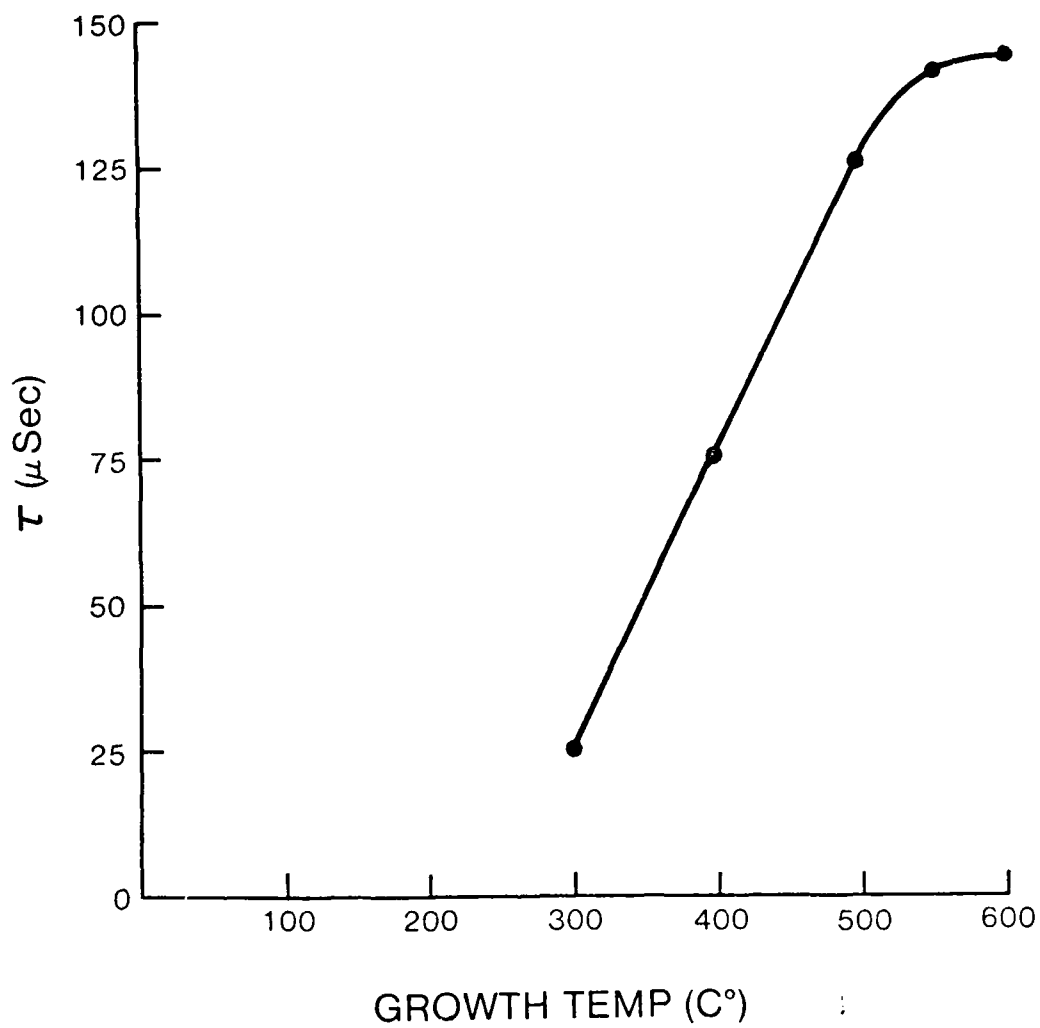


Figure 1. Growth temperature vs. lifetime for NPP crystals.

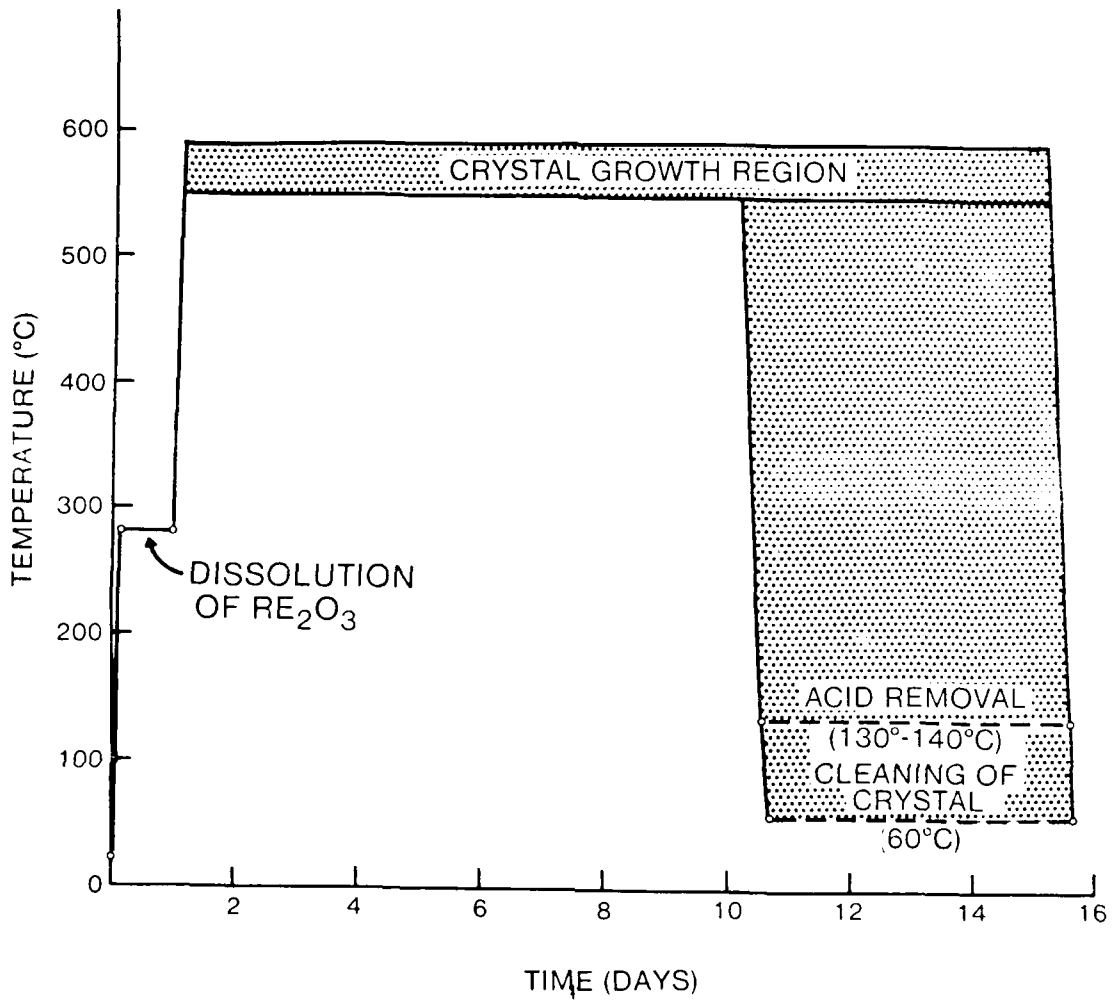


Figure 2. Time vs. temperature for growth of NPP crystals.

melt using very low pull rates (Fig. 3). The linear displacement transducer of the puller not only enables the measurement and recording of the stability of the pulling rate but also precise repositioning of the seed within $\pm 2 \mu\text{m}$. Rotation of the seed is varied between 10 and 60 rpm. The composition of the fluxed melt in our preliminary growth experiments in mol ratios for $\text{LiO}_2:\text{Nd}_2\text{O}_3:\text{P}_2\text{O}_5$ is 3:1:6. The temperature at the melt surface is varied between 870°C and 950°C , and the temperature gradient between the surface and bottom of the melt is between 1°C and 5°C while the pulling rate is varied between 80 and $150 \mu\text{m/hr}$.

Figure 4 is a photograph of an LNP crystal (~ 1 cm in diameter) pulled under such conditions by top seeding. Growth rate in the b-direction of LNP crystals is about twice as fast as in the other directions; crystals grown in this direction are of the best quality. Major difficulties are inclusions in the crystals as well as multiple nucleation. Seeds are now being grown and fabricated which will allow crystal growth in the b-direction.

2.3 $\text{NdAl}_3(\text{BO}_3)_3\text{-}_4$ (NAB)

Our studies of the NAB crystals indicate that it would be extremely difficult to grow single crystals of good optical quality and large enough for fabrication of laser rods. Recent studies by other workers of the crystal structure of NAB produced contradictory results with respect to the single or multiple-phase nature of these crystals. We have therefore discontinued our crystal growth experiments on NAB until the structure problem has been resolved.

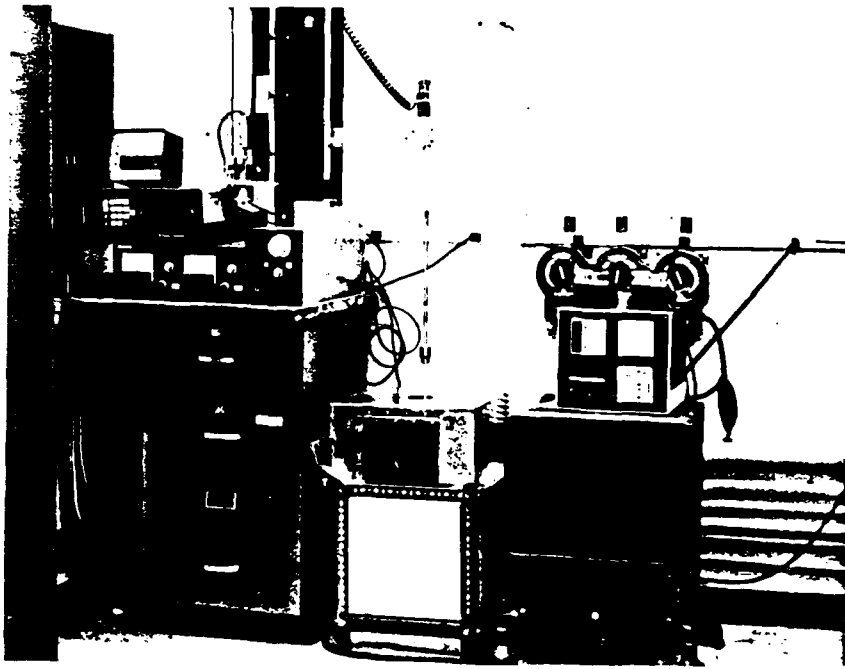


Figure 3. Pulling system for top-seeded flux growth of LNP crystals.

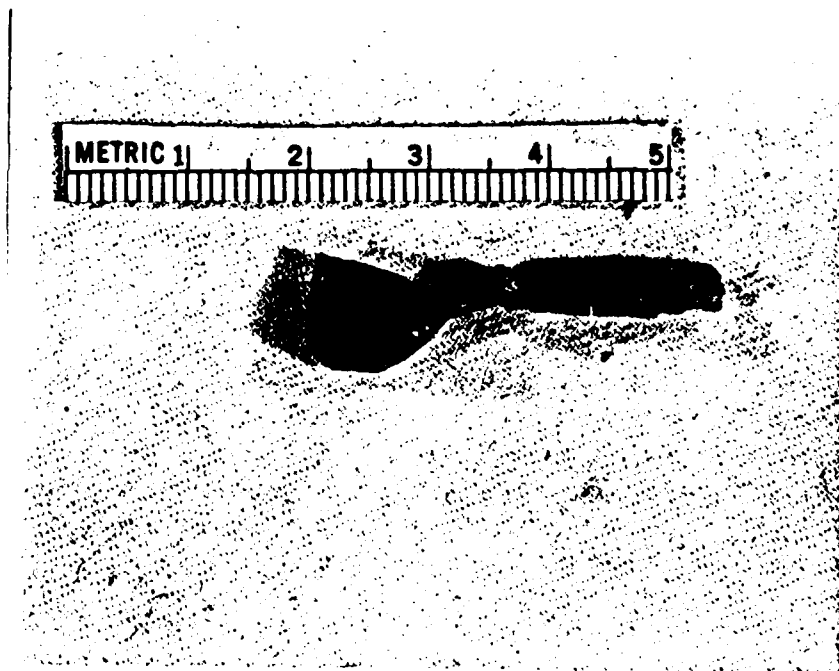


Figure 4. LNP crystal grown by top-seeded flux growth method.

3. OPTICAL CHARACTERIZATION OF LASER MATERIALS

3.1 Emission Spectra

The emission spectra of Nd^{3+} ions in NPP, LNP, and NAB crystals have been obtained between $9000\text{-}11750\text{ cm}^{-1}$ at both room and liquid-nitrogen temperatures. Figures 5, 6, 7 show the room-temperature data for the three crystals; the temperature-broadened ${}^4\text{F}_{3/2} \rightarrow {}^4\text{I}_{11/2}$, and ${}^4\text{F}_{3/2} \rightarrow {}^4\text{I}_{9/2}$ lines are used in the emission cross section calculations that follow. Figure 8, 9 shows the data at liquid-nitrogen temperature for NPP and LNP, together with the level assignment corresponding to various Stark components in NPP. The spectra compare well with the published data [Refs. 1,2,3]. The wavelengths at which peak ${}^4\text{F}_{3/2} \rightarrow {}^4\text{I}_{11/2}$ emission occurs are obtained from our room-temperature data. These peaks are indicated on Figures 5, 6, 7 for the three crystals together with the corresponding published [Refs. 1,2,3] values in parenthesis.

3.2 Emission Cross Sections

Emission cross sections at the peak fluorescence lines ${}^4\text{I}_{11/2}$ of Nd^{3+} in the three different crystal matrices were determined by comparing the intensities of these lines to the lines at the ground ${}^4\text{I}_{9/2}$ levels whose cross sections were determined from absorption measurements. For this purpose, we obtained detailed transmission spectra near the ${}^4\text{I}_{9/2} \rightarrow {}^4\text{F}_{3/2}$ absorption lines; these are given in Figures 10, 11, 12. The absorption cross sections are calculated approximately by using the relation:

$$I_{\text{out}}/I_{\text{in}} = e^{-\sigma_a N \ell} \quad (1)$$

where $I_{\text{out}}/I_{\text{in}}$ = transmission at a line well separated from others, σ_a = absorption cross section, N = concentration of Nd^{3+} ions calculated by using Boltzmann distribution, and ℓ = length of crystal in the propagation direction. The emission cross section is then calculated from [Ref. 4]:

$$\sigma_e = \sigma_a \left(\frac{N_a}{N_e} \right)^2 \left(\frac{\lambda_e}{\lambda_a} \right)^5 \left[\left(\frac{dI}{d\lambda} \right)_e / \left(\frac{dI}{d\lambda} \right)_a \right] \quad (2)$$

where, σ = cross section, n = index of refraction, λ = free space wavelength, and $(dI/d\lambda)$ = peak emission power per unit wavelength interval. Subscripts e and a are used to indicate emission and absorption processes, respectively. The ratio $[(dI/d\lambda)_e/(dI/d\lambda)_a]$ is obtained for each crystal from the spectra given in Figures 5, 6, 7. The resultant absorption and emission cross sections, together with the wavelengths at which they were calculated, are given in Table 1.

TABLE 1: Absorption and Emission Cross Sections.

Crystal	λ_a	σ_a	λ_e	σ_e
NPP	865	1.42×10^{-20}	1049	2.4×10^{-19}
LNP	871	1.25×10^{-20}	1046	2.5×10^{-19}
NAB	900	6.8×10^{-20}	1060	6.5×10^{-19}

λ_a, λ_b wavelength at which absorption and emission cross sections are defined (nm).

σ_a, σ_e absorption, and emission cross sections (cm^2).

3.3 Basic Spectroscopic and Laser Properties of Crystals

This section summarizes the preliminary results of the evaluation on the optical properties of NPP, LNP, and NAB. The fluorescence lifetime of $\text{Nd}^{3+} \ 4F_{3/2} \rightarrow 4I_{11/2}$ levels and corresponding emission cross sections are given in Table 2 for the three materials.

TABLE 2: Optical and Laser Properties of Crystals.

Crystal	τ	σ_e	$(\sigma_e \tau)$	E_T	E_{out}
NPP	140	2.4×10^{-19}	3.36×10^{-23}	0.42	33
LNP	140	2.5×10^{-19}	3.5×10^{-23}	0.40	34
NAB	16	6.5×10^{-20}	1.04×10^{-23}	1.40	24

τ = fluorescence lifetime of $4F_{3/2} \rightarrow 4I_{11/2}$ line (μsec)

σ_e = emission cross section of $4F_{3/2} \rightarrow 4I_{11/2}$ line (cm^2)

$(\sigma_e \tau)$ = threshold parameter [Ref. 5] (sec-cm^2)

E_T = threshold energy for pulsed operation (Joules)

E_{out} = output energy for 4 Joules input electrical energy (Joules)

The lifetime data was taken from our previous measurements on the same crystals. In the table, we give the factor ($\sigma_e \tau$), which is a parameter determining the threshold pump density, and the pump threshold for pulsed operation. The importance of these parameters is discussed in Reference 5. The threshold energy, E_T , was obtained by assuming a 2% pumping efficiency (see Eq. 3), 65% reflective output mirror, 2% internal losses, a crystal with 2 x 2 mm area, and a pumping pulse duration of 80 μ sec. The output energy, E_{out} , was obtained by assuming a 4 Joule electrical input energy with the same parameters mentioned above. For calculations, a quasi cw analysis as described in Ref. 5 was used.

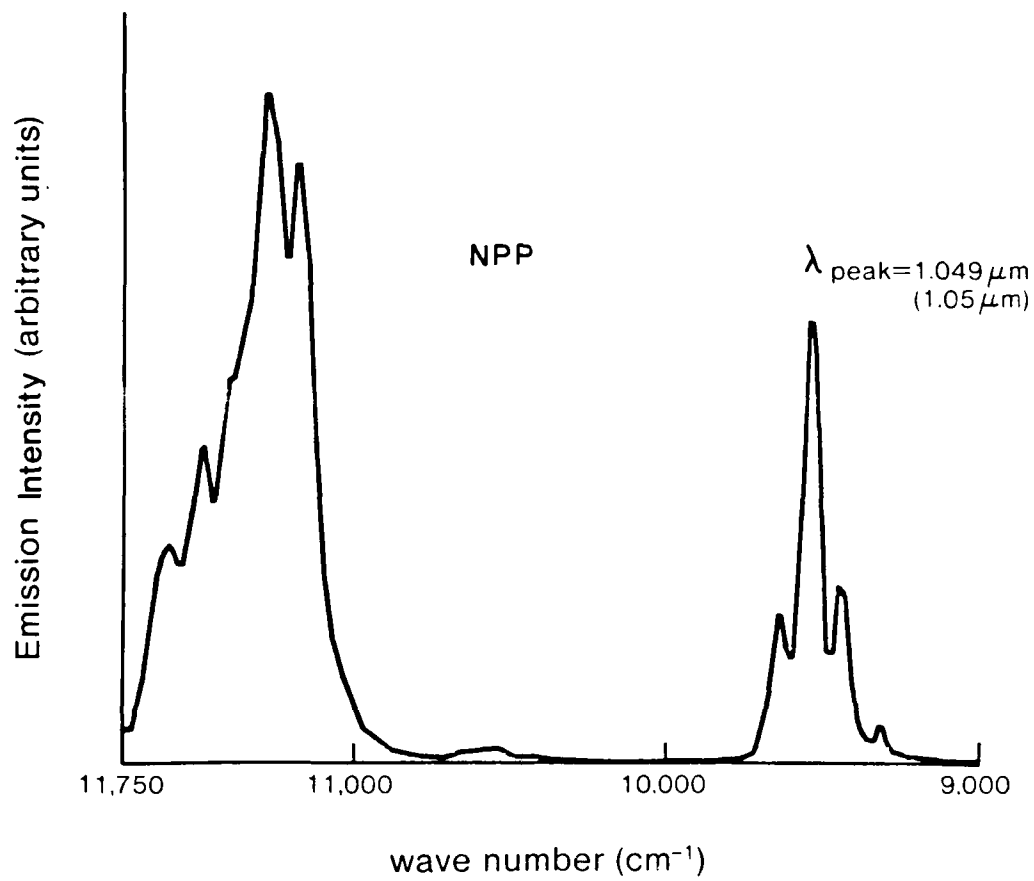


Figure 5. Room-temperature emission spectrum of Nd³⁺ in NPP. Peak emission wavelength is indicated. Value in parenthesis was taken from Ref. 1.

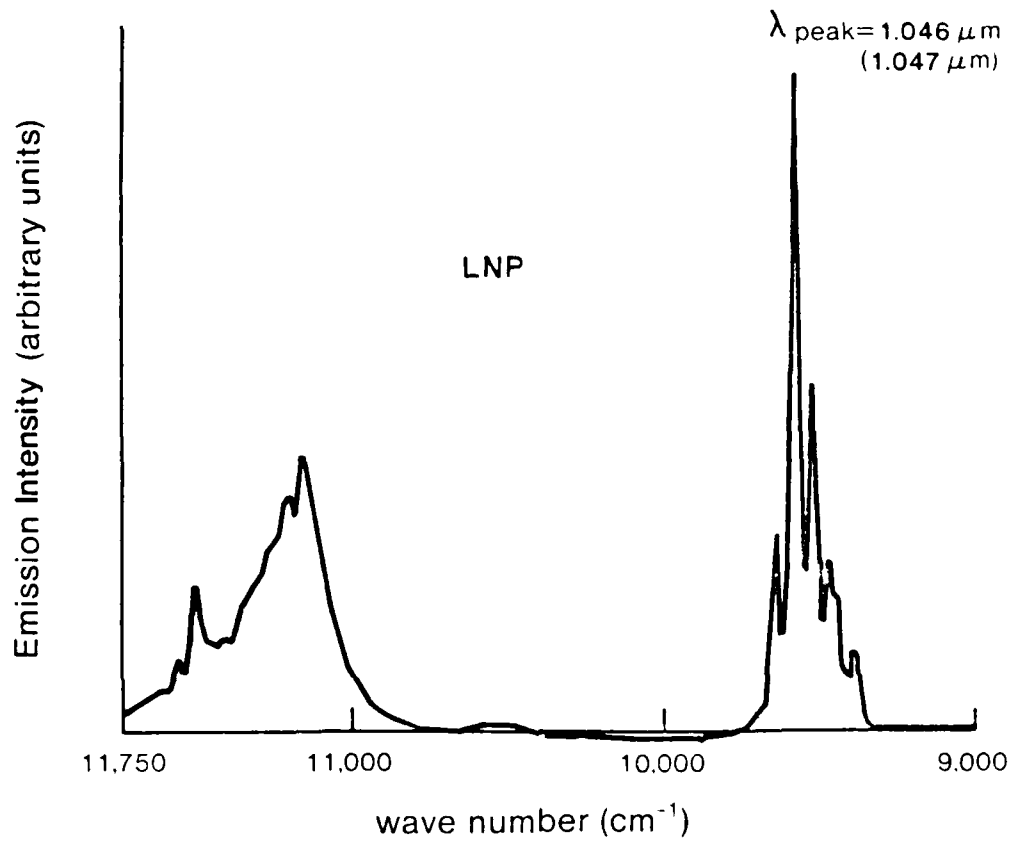


Figure 6. Room-temperature emission spectrum of Nd³⁺ in LNP. Peak emission wavelength is indicated. Value in parenthesis was taken from Ref. 2.

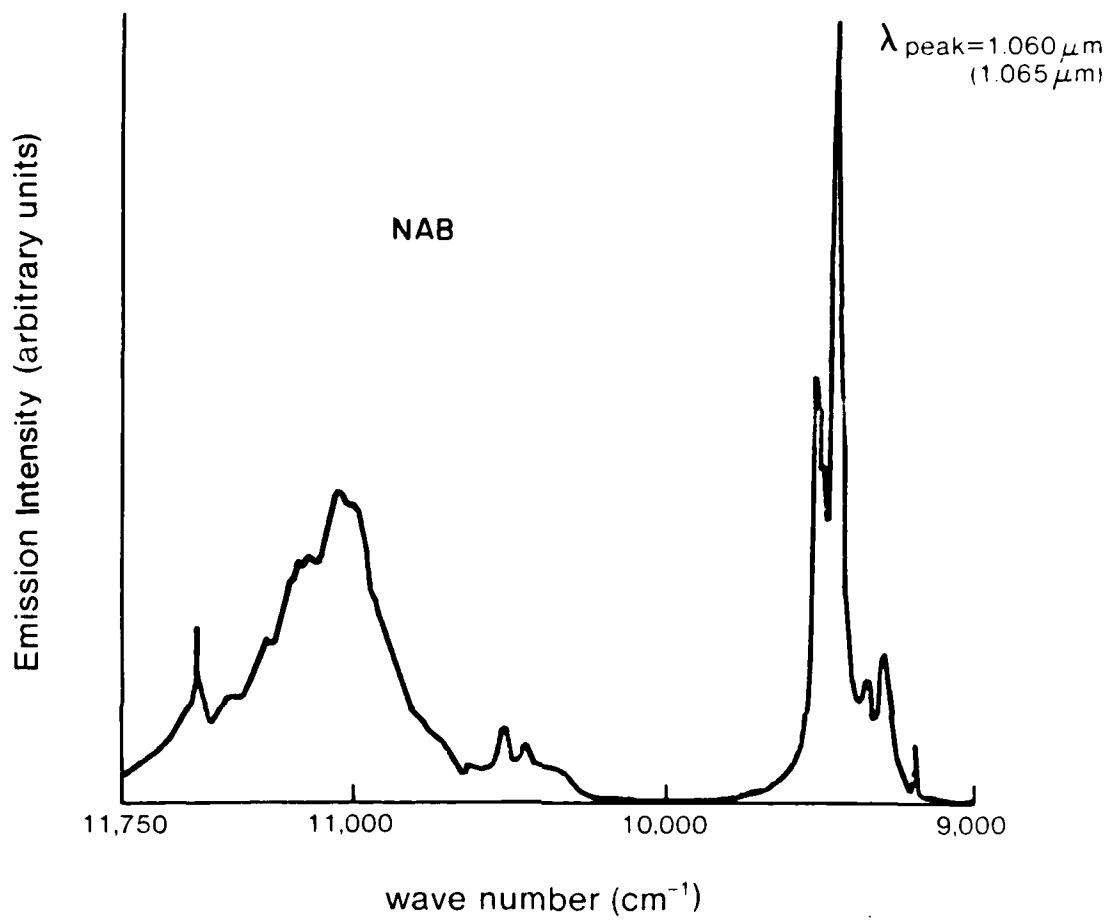


Figure 7. Room-temperature emission spectrum of Nd³⁺ in NAB. Peak emission wavelength is indicated. Value in parenthesis was taken from Ref. 3

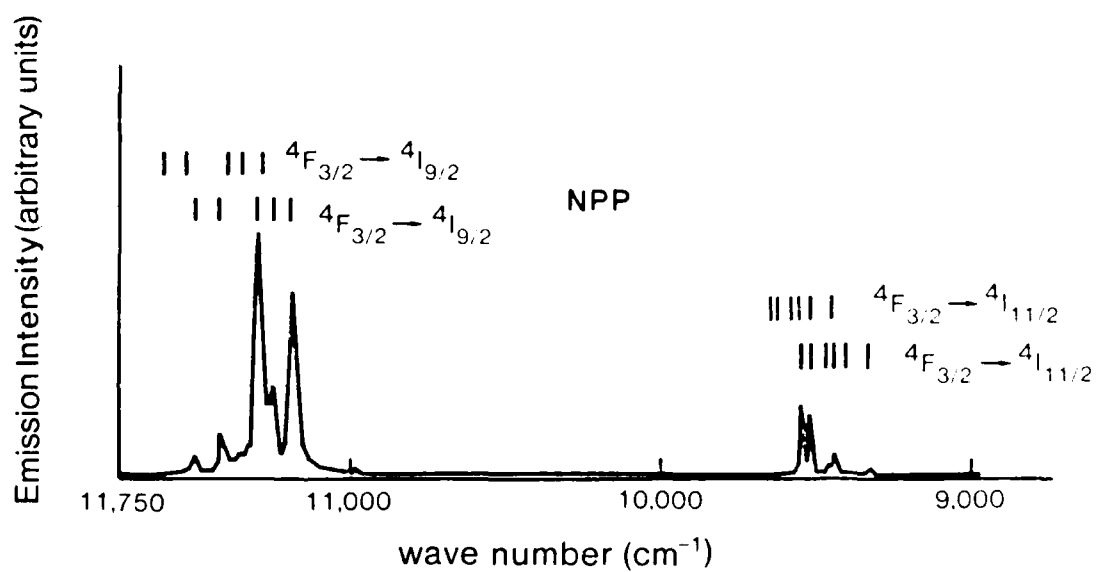


Figure 8. Liquid-nitrogen temperature emission spectrum of Nd^{3+} in NPP. The levels are assigned for the transitions from $4F_{3/2}$ doublet to $4I_{11/2}$ and $4I_{9/2}$ multiplets in NPP.

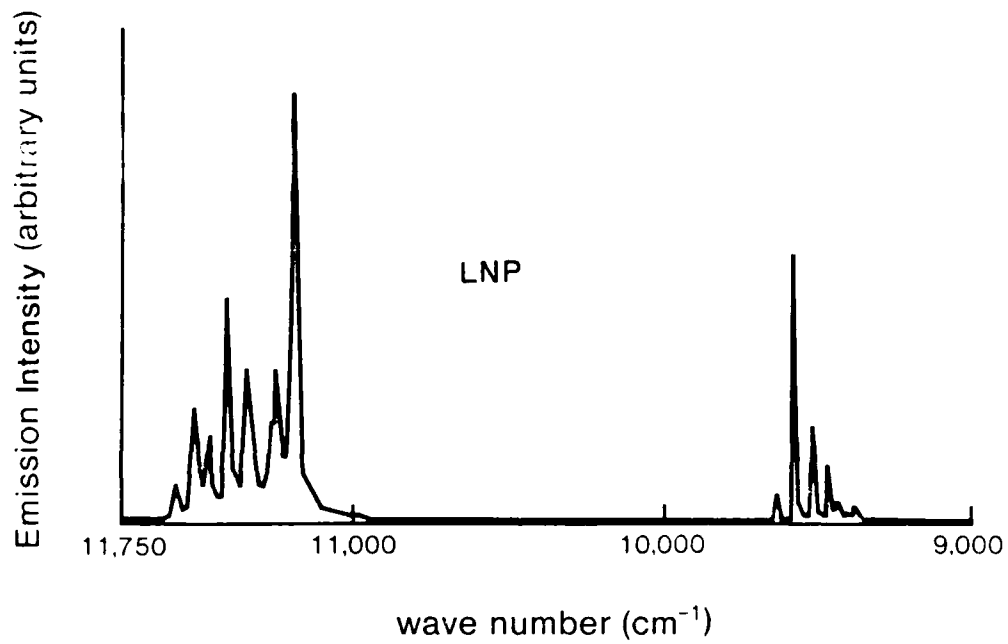


Figure 9. Liquid-nitrogen temperature emission spectrum of Nd³⁺ in LNP.

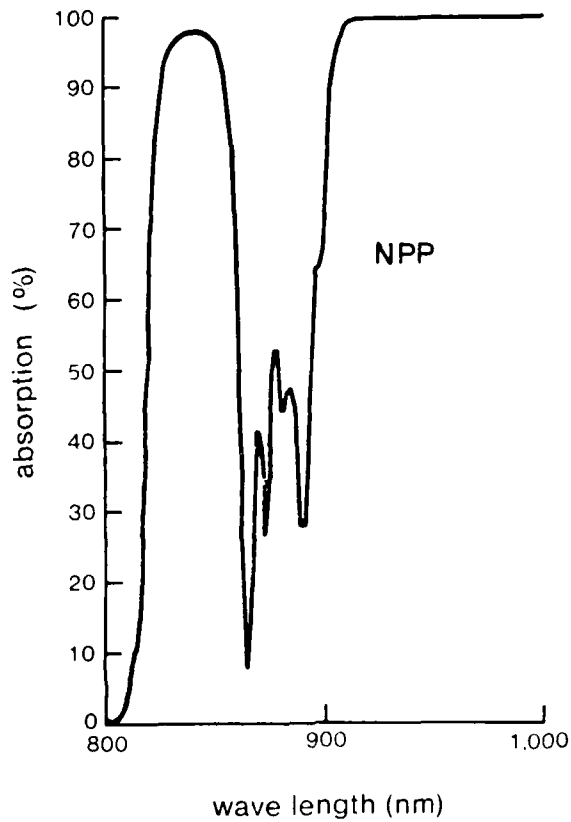


Figure 10. Absorption spectrum of NPP near ${}^4I_{9/2} \rightarrow {}^4F_{3/2}$ transition to be used in calculating emission cross section.

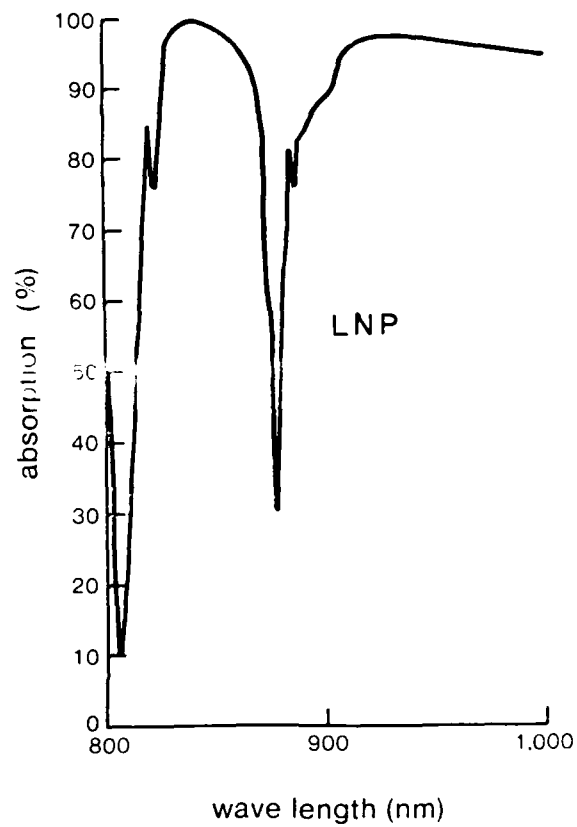


Figure 11. Absorption spectrum of LNP near ${}^4I_{9/2} \rightarrow {}^4F_{3/2}$ transition to be used in calculating emission cross section.

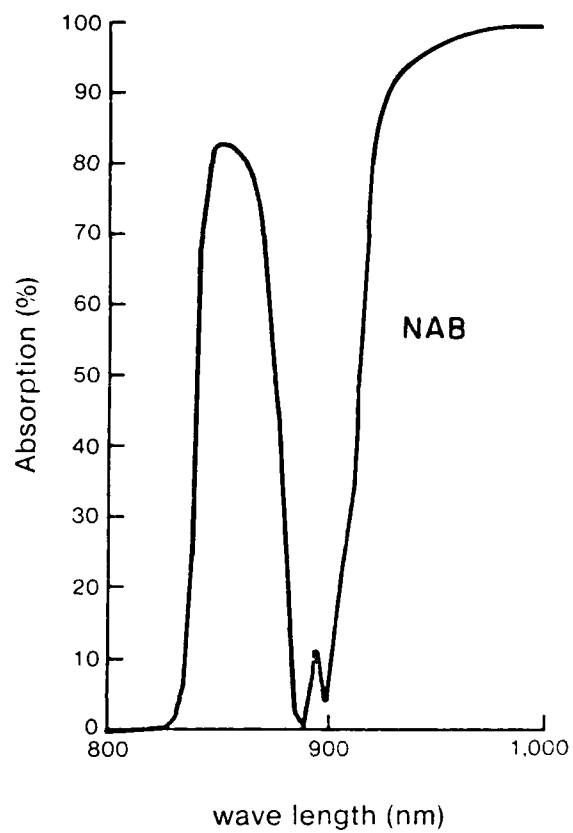


Figure 12. Absorption spectrum of NAB near ${}^4I_{9/2} \rightarrow {}^4F_{3/2}$ transition to be used in calculating emission cross section.

4. LASER PERFORMANCE OF NPP

Previously, random measurements were made to test the behavior of the NPP laser in our experimental laser setup. These measurements were not enough to indicate the conditions which optimize the laser output. Recently, however, we completed a set of measurements on the output energy versus input energy characteristics of this NPP laser with two different pump cavities and with various mirrors. The results of this study are summarized in Figures 13, 14, 15. Figures 13 and 14 give the characteristics for a double elliptical cavity with two and one lamp (failure mode) flashing, respectively, and with flat output mirrors of 85% and 75% reflectivity. Figure 15 gives the output behavior for a single elliptical cavity with an 85% reflective flat output mirror. In all measurements, the highly reflective back mirror had a radius of curvature of 10 cm, the front mirror was 2x2x20 mm, and the length of the cavity was 9 cm. These results show that it is more efficient to pump with a single flash lamp in both pump cavities than to pump with a double lamp. This shows the inefficiency of the lamp design at the low energies which are of interest for the miniature laser, and may also explain the relatively large input energies necessary to obtain a given output energy. From the data for the double elliptical pumping cavity, it is seen that a slightly higher output is obtained for a 75% reflective output mirror.

The slope efficiencies for the double elliptical cavity with two lamps and output couplings of 75% and 85% were found to be about 0.22% and 0.20%, respectively. The approximate expression for the slope efficiency is given by:

$$\frac{d E_{out}}{d E_{in}} = \eta_p \left(1 + \frac{L}{T} \right)^{-1} \quad (3)$$

where E_{out} , E_{in} = energies for laser output and optical input, η_p = effective overall pumping efficiency, L = internal laser losses, and T = output mirror transmission. Using the ratio of Eq. (3) for the two different output mirrors mentioned above, the total internal laser loss is

calculated to be about 5%. Using this value in Eq. (3), the overall pumping efficiency is found to be about 0.25%. With these parameters and a crystal area of $2 \times 2 \text{ mm}^2$, we calculated [Ref. 5] that the threshold energy for the laser with a $140 \mu\text{sec}$ pump pulse length should be about 2.2 Joules. This value is close to half of what we observed, and still much larger than the case given as E_T in Table 2. This is another indication of the inefficiency of the flash lamps used, especially at the lower pulse energies we are interested. Also, due to the large size of these flash lamps, the pump cavity does not operate at an optimum, closely coupled condition.

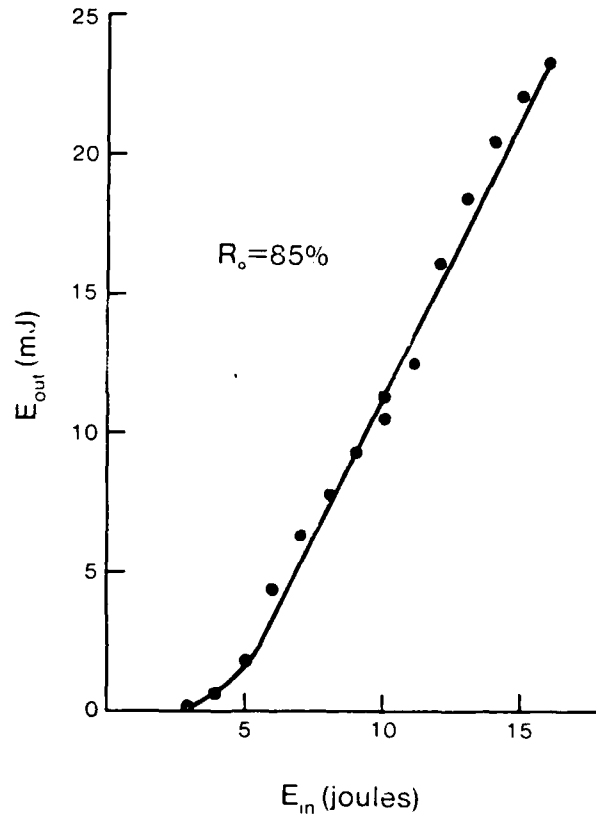
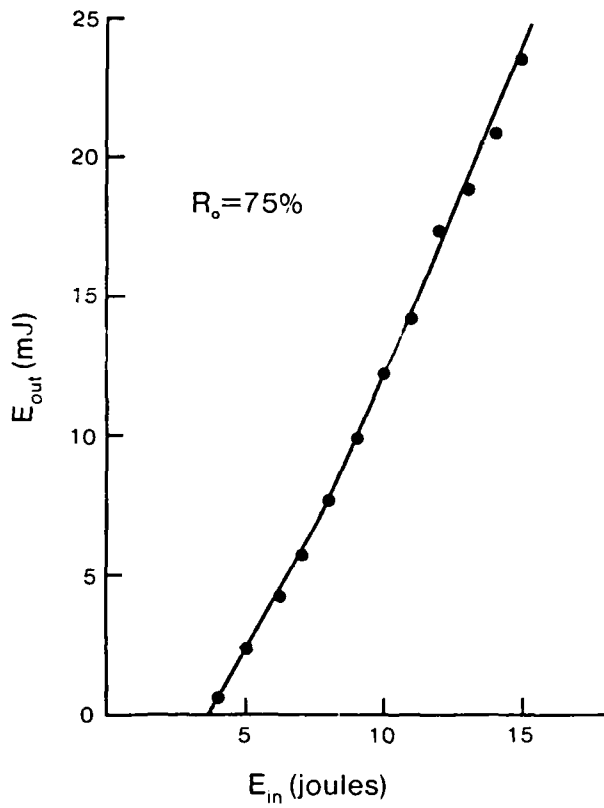


Figure 13. Light output energy vs. electrical input energy for NPP laser in a double elliptical pumping cavity with two flash lamps and output mirror reflectivities of 75% and 85%.

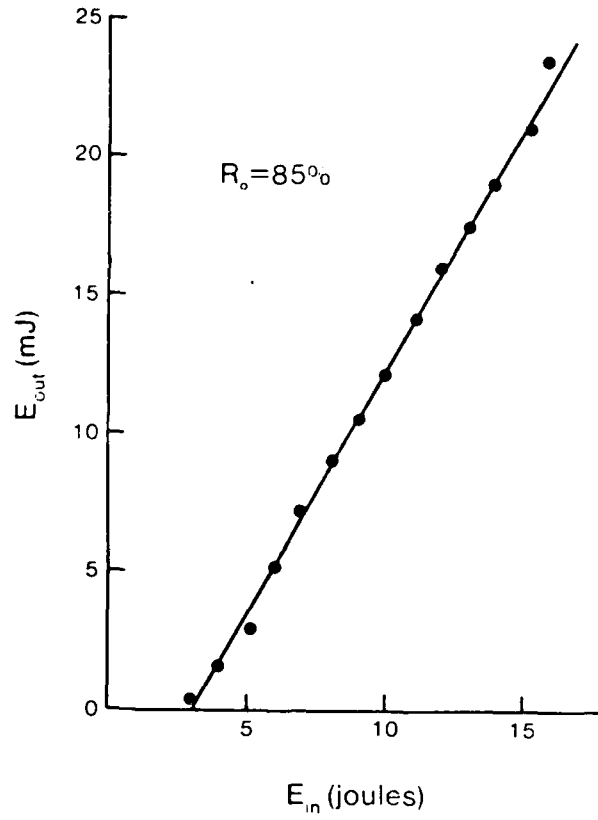
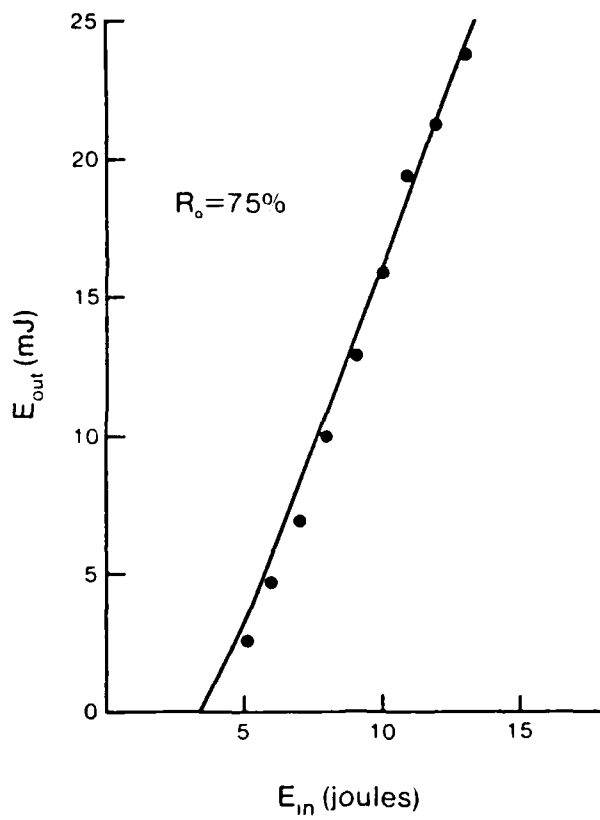


Figure 14. Light output energy vs. electrical input energy for NPP laser in a double elliptical pumping cavity with one flash lamp (failure mode) and output mirror reflectivities of 75% and 85%.

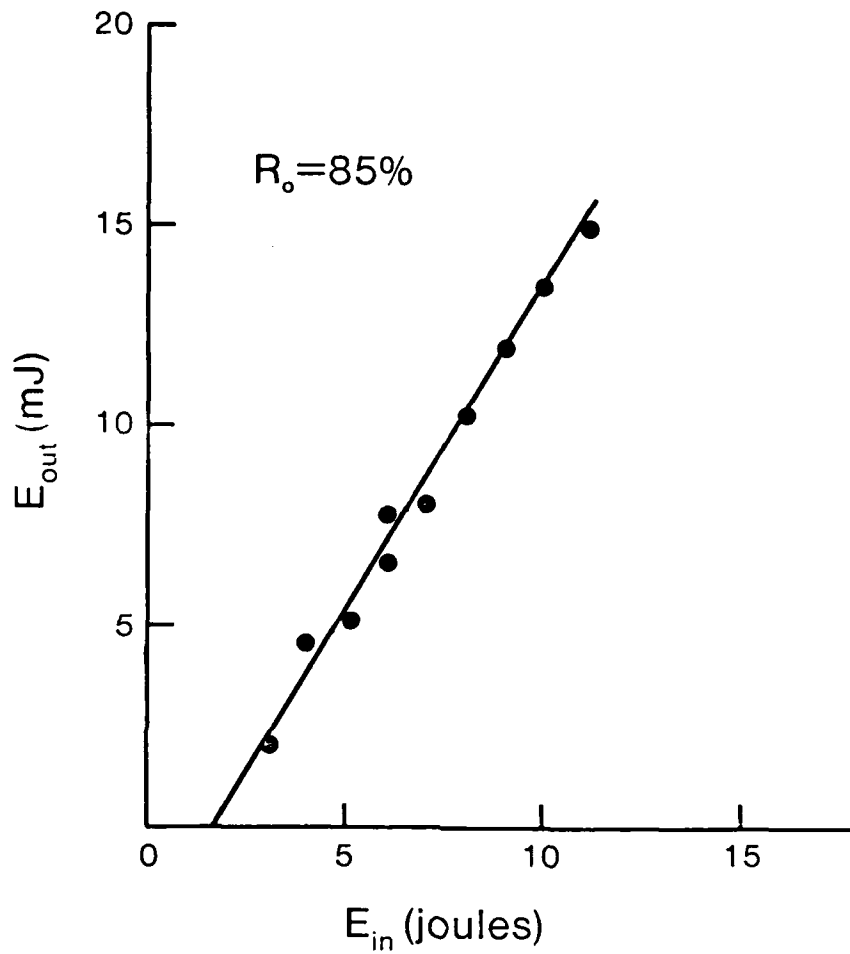


Figure 15. Light output energy vs. electrical input energy for NPP laser in a single elliptical cavity with 85% reflective output mirror.

5. PLANS FOR NEXT QUARTER

- a. Continue growth of large NPP crystals of high optical quality and fabricate laser rods.
- b. Investigate growth methods for stoichiometric Er^{3+} crystals and produce small crystals for evaluation.
- c. Build miniature laser system from completed design and test with NPP crystals.
- d. Test thermal effects on NPP laser.
- e. Obtain a Q-switch material and test with NPP laser.
- f. Study Er^{3+} fluorescence and laser properties in the eye-safe region of the spectrum ($1.56 \mu\text{m}$).

6. REFERENCES

1. M. Blätte, H.G. Danielmeyer, R. Ulrich; Appl. Phys. 1, 275 (1973).
2. K. Otsuka, T. Yamada, M. Saruwatari, T. Kimura; IEEE JOE 11, 330 (1975).
3. S.R. Chinn, H.Y-P Hong; Opt. Comm. 15, 345 (1975).
4. S. Singh, R.G. Smith, L.G. Van Uitert; Phys. Rev. B 10, 2566 (1974).
5. G. Huber, Current Topics in Materials Science, Vol. 4, Ed. E. Kaldis, North Holland, p. 23, (1980).

DISTRIBUTION LIST

	<u>Copies</u>
Director Defense Advanced Research Projects Agency Attention: TIO/Admin. 1400 Wilson Blvd. Arlington, Virginia 22314	(3)
Dr. Jefferey L. Paul DELNV-L Night Vision & Electro-Optics Laboratories Fort Belvoir, Virginia 22060	(1)
Defense Documentation Center Cameron Station Alexandria, Virginia 22314	(12)
TACTEC Battelle Memorial Institute 505 King Avenue Columbus, Ohio 43201	(1)

END
FILMED
FEB. 1988
DTIC